



HAL
open science

A multidimensional H-1 NMR lipidomics workflow to address chemical food safety issues

Jérémy Marchand, Estelle Martineau, Yann Guitton, Bruno Le Bizec, Gaud Dervilly-Pinel, Patrick Giraudeau

► **To cite this version:**

Jérémy Marchand, Estelle Martineau, Yann Guitton, Bruno Le Bizec, Gaud Dervilly-Pinel, et al.. A multidimensional H-1 NMR lipidomics workflow to address chemical food safety issues. *Metabolomics*, 2018, 14 (5), pp.1-11. 10.1007/s11306-018-1360-x . hal-02625035

HAL Id: hal-02625035

<https://hal.inrae.fr/hal-02625035v1>

Submitted on 25 Nov 2024

HAL is a multi-disciplinary open access archive for the deposit and dissemination of scientific research documents, whether they are published or not. The documents may come from teaching and research institutions in France or abroad, or from public or private research centers.

L'archive ouverte pluridisciplinaire **HAL**, est destinée au dépôt et à la diffusion de documents scientifiques de niveau recherche, publiés ou non, émanant des établissements d'enseignement et de recherche français ou étrangers, des laboratoires publics ou privés.

1 **A multidimensional ¹H NMR lipidomics workflow to address chemical food**
2 **safety issues**

3

4 Jérémy Marchand^{a,b}, Estelle Martineau^{a,c}, Yann Guitton^b, Bruno Le Bizec^b,

5 Gaud Dervilly-Pinel^{b,*}, Patrick Giraudeau^{a,d,*}

6 a. EBSI Team, Chimie et Interdisciplinarité : Synthèse, Analyse, Modélisation (CEISAM)
7 Université de Nantes, CNRS, UMR 6230, BP 92208, 2 rue de la Houssinière, 44322 Nantes
8 (France).

9 b. Laberca, Oniris, INRA, Université Bretagne Loire, 44307, Nantes-FR.

10 c. SpectroMaitrise, CAPACITES SAS, 26 Bd Vincent Gâche, 44200 Nantes (France)

11 d. Institut Universitaire de France. 1 rue Descartes 75005, Paris Cedex 05 (France)

12

13

14 * Corresponding authors:

15 Gaud Dervilly-Pinel (gaud.dervilly@oniris-nantes.fr)

16 Patrick Giraudeau (patrick.giraudeau@univ-nantes.fr)

17

18

19 **Abstract**

20 *Introduction.* Although it is still at a very early stage compared to its mass spectrometry (MS)
21 counterpart, Proton Nuclear Magnetic Resonance (NMR) lipidomics is worth being investigated as an
22 original and complementary solution for lipidomics. Dedicated sample preparation protocols and
23 adapted data acquisition methods have to be developed to set up an NMR lipidomics workflow; in
24 particular, the considerable overlap observed for lipid signals on 1D spectra may hamper its
25 applicability.

26 *Objectives.* The study describes the development of a complete proton NMR lipidomics workflow for
27 application to serum fingerprinting. It includes the assessment of fast 2D NMR strategies, which,
28 besides reducing signal overlap by spreading the signals along a second dimension, offer compatibility
29 with the high-throughput requirements of food quality characterization.

30 *Methods.* The robustness of the developed sample preparation protocol is assessed in terms of
31 repeatability and ability to provide informative fingerprints; further, different NMR acquisition
32 schemes –including classical 1D, fast 2D based on non-uniform sampling or ultrafast schemes– are
33 evaluated and compared. Finally, as a proof of concept, the developed workflow is applied to
34 characterize lipid profiles disruption in serum from β -agonists diet fed pigs.

35 *Results.* Our results show the ability of the workflow to discriminate efficiently sample groups based
36 on their lipidic profile, while using fast 2D NMR methods in an automated acquisition framework.

37 *Conclusion.* This work demonstrates the potential of fast multidimensional ^1H NMR –suited with an
38 appropriate sample preparation– for lipidomics fingerprinting as well as its applicability to address
39 chemical food safety issues.

40 **Keywords**

41 Lipidomics; NMR fingerprinting; Ultrafast NMR; Non Uniform Sampling; Serum; Food quality

43 1 Introduction

44 Over the last decade, the growth of lipidomics, defined as “the full characterization of lipid molecular
45 species and of their biological roles with respect to expression of proteins involved in lipid metabolism
46 and function, including gene regulation” (Spener *et al.*, 2003), has been noteworthy. It encountered a
47 revival of research works thanks to recent advances in both analytical chemistry and data analysis,
48 which greatly accelerated progresses in the field. Lipidomics is now considered a relevant approach for
49 addressing a broad range of research questions, as attested by the large number of review articles
50 dedicated to the topic (Bou Khalil *et al.*, 2010; Cajka and Fiehn, 2014; Hyotylainen *et al.*, 2017; Li *et al.*,
51 2014; Wenk, 2005, 2010; Yang and Han, 2016). The applications of this field of research are diverse
52 and include disease biomarker discovery, drug development, drug safety assessment, nutrition or plant
53 research (Zhao *et al.*, 2014). Some studies also showed its potential as a tool for the assessment of
54 food quality; authenticity applications in particular have been widely reported (Li *et al.*, 2017). In
55 chemical food safety, lipidomics-based strategies are also relevant, both at the risk analysis and
56 management steps, for instance for the control of forbidden growth promoting agents in livestock
57 (Nzougnet *et al.*, 2015). It is worth noting that most of the reported lipidomics studies use Mass
58 Spectrometry (MS) as a fingerprinting analytical strategy, often hyphenated to liquid chromatography.
59 Although MS allows sensitive measurement of hundreds of species in a single scan (Veenstra, 2012), it
60 is a destructive technique, which suffers from the various capabilities of ionization between lipid
61 species. Nuclear Magnetic Resonance (NMR), in contrast, does not induce degradation of the sample
62 upon analysis and is a highly reproducible and directly quantitative technique in spite of its lower
63 sensitivity. NMR is therefore a very promising tool for lipidomics, as illustrated by a recent perspective
64 on the subject (Li *et al.*, 2017). Moreover, covering the wide range of lipid species with one single
65 untargeted MS method is difficult (Lee and Yokomizo, 2018) and NMR lipidomics could be a useful
66 complementary strategy for identifying the discriminant lipid classes.

67 However, even though a few studies reported the use of ^1H NMR for lipidomics (Beger *et al.*, 2006;
68 Ekman *et al.*, 2009; Fernando *et al.*, 2011), this technique is still minor in the field (Cajka and Fiehn,
69 2014; Li *et al.*, 2014). The reasons for this lack of popularity are diverse. First of all, 1D ^1H NMR spectra
70 suffer from severe peak overlaps, which hinder the accurate determination of peak areas (Giraudeau,
71 2017). Heteronuclear NMR such as ^{13}C NMR is considered an interesting alternative as it offers a better
72 resolution of the NMR signals, thanks to the large bandwidth involved. Indeed, ^{13}C NMR has been used
73 for decades in the analysis of lipids, for instance to determine the composition of fatty acids in food
74 samples (Mavromoustakos *et al.*, 1997; Vlahov, 1997). Nevertheless, such method suffers from a poor
75 sensitivity compared to ^1H , due to the low abundance of ^{13}C (1.1% at natural abundance) and to the
76 low gyromagnetic ratio of this nucleus –although the latter can be circumvented by indirect detection
77 methods (Merchak *et al.*, 2017). Interestingly, ^{31}P NMR has also been reported for lipidomics (Li *et al.*,
78 2017) but does not allow the analysis of global lipid fingerprint, as it focuses on the determination of
79 phospholipids.

80 Alternatively, 2D ^1H NMR is an appealing solution in order to obtain a better resolution of the lipid
81 signals without sacrificing the sensitivity, as it allows to spread the signals on a 2D plane. Such
82 experiments are however difficult to apply to lipidomics, as they involve long experiments –up to
83 several hours of acquisition– which do not meet the high-throughput requirements associated with
84 omics approaches. Moreover, the absolute quantification is not straightforward and thus requires
85 specific and time-consuming acquisition schemes or calibration procedures (Giraudeau, 2014).

86 Fortunately, fast 2D NMR approaches have emerged to tackle the issue of acquisition time (Rouger *et al.*
87 *et al.*, 2017). Two of these approaches, ultrafast (UF) NMR and non-uniform sampling (NUS) have already
88 shown great potential and usefulness in the field of metabolomics (Marchand *et al.*, 2017), either used
89 for fingerprinting (Le Guennec *et al.*, 2014) or associated with a calibration procedure for targeted
90 analyses (Jézéquel *et al.*, 2015) when absolute quantification is necessary.

91 Based on such developments, fast 2D NMR could also be relevant within NMR-based lipidomics
92 workflows. However, in order to use such strategies on a routine basis, there is a need for the
93 development and testing of a suitable and comprehensive workflow, including a repeatable sample
94 preparation protocol and an efficient fingerprinting method. In this perspective, we have set up a
95 complete strategy for serum lipidomics. First a sample preparation procedure was developed and
96 assessed in terms of repeatability, a critical characteristic for the ultimate comparison of the samples.
97 Then two different fast 2D ^1H NMR techniques for untargeted lipidomics fingerprinting were
98 experimented and their performances were compared to 1D ^1H NMR. Finally, to evaluate the capacity
99 of the developed approach to address key challenges in NMR lipidomics –namely exploitability, wealth
100 of information and relevance with regard to research question raised– we applied the protocol to a
101 current chemical food safety issue: the detection of forbidden vet drugs administration in livestock. In
102 that context and as a proof of concept, serum samples from ractopamine diet fed pigs have been
103 characterized and their lipids fingerprints compared to control ones with the objective of highlighting
104 specific patterns. Such a set of serum samples ($n > 40$) was obtained in a well-controlled animal
105 experiment which already enabled reporting specific patterns when investigating the polar fraction of
106 the metabolome by MS-metabolomics (Peng *et al.*, 2017). Subsequent data processing and analysis
107 enabled describing specific lipidomics patterns upon NMR fingerprinting associated to ractopamine
108 treated animals, as could be expected upon the use of such growth promoter (Guitton *et al.*, 2017).

109 **2 Materials and Methods**

110 The detailed experimental protocol (sample preparation, NMR data acquisition and processing, data
111 analysis) is provided as Supplementary Material. We will focus here on the most critical points of the
112 workflow.

113 **2.1 Animal experiment/samples**

114 Blood samples were collected from an ethically approved experiment described elsewhere (Peng *et*
115 *al.*, 2017) and involving ten four-month-old female pigs randomly divided in control and treated

116 groups, the latter one being daily exposed to Ractopamine hydrochloride (Sigma Aldrich) through feed
117 (10 ppm). **Four** QC samples consisting of all the collected samples pooled in identical quantities and
118 mixed together, were prepared. All serum samples were aliquoted and stored at -20°C before analysis.

119 **A schematic of this design can be found in Supplementary Fig. 3.**

120 For all preliminary sample preparation optimization steps, a serum mix constituted from routine pig
121 blood tests was used as matrix reference.

122 **2.2 Solvents, chemicals**

123 Details on the solvent and chemicals used for extraction/analysis can be found in Supplementary
124 Material.

125 **2.3 Sample preparation**

126 The lipidic fraction was obtained from serum (sample size 300 µL) according to a modified Bligh and
127 Dyer extraction, inspired from ~~Kouassi~~ Nzoughet (Nzoughet *et al.*, 2015). The final extracts were
128 suspended in 700 µL of CDCl₃ containing 0.3 mmol/L of dimethylsulfone (DMSO₂) as an internal
129 standard.

130 **2.4 NMR Analysis**

131 All the spectra were automatically recorded using IconNMR (Bruker Biospin) on a 16.4 T Bruker Avance-
132 III HD spectrometer operating at a ¹H frequency of 700.13 MHz, equipped with an inverse ¹H/¹³C/¹⁵N/²H
133 cryogenically cooled probe. The sample temperature was set at 298 K and a SampleJet auto-sampler
134 set at 277 K, requiring 4 inches long NMR tubes in 96-well plates was used. 1D ¹H, 2D ¹H NUS ZQF-
135 TOCSY and 2D ¹H UF COSY spectra were separately acquired. Acquisition and processing parameters
136 are detailed in Supplementary Material.

137 **3 Results and discussion**

138 **3.1 Sample preparation**

139 As described in Fig. 1, the first step of the lipidomics workflow aims at extracting the lipidic fraction of
140 the samples in a repeatable way so that they can eventually be compared, while eliminating interfering
141 signals such as those from proteins. Therefore, it is crucial to check the repeatability of this step and
142 the apparent composition of the resulting fraction, *via* NMR spectra observation. To this aim, the same
143 reference serum mix was extracted four different times, using the modified Bligh and Dyer protocol
144 described in Supplementary Material. The four NMR tubes were thus submitted to 1D ¹H analysis (see
145 Supplementary Material for the detailed parameters of acquisition, processing and integration) in
146 identical conditions. Since 1D NMR is considered repeatable at *ca.* 1% for signal-to-noise ratio (SNR)
147 values higher than 50 (Barding *et al.*, 2012; Malz, 2008), any variation observed across the four
148 resulting NMR spectra above this value is mainly expected to reflect the repeatability of the
149 preparation step, provided that the observed signals are intense enough. The spectra (Supplementary
150 Fig. 1, top) obtained for these samples showed a rich fingerprint with characteristic signals mainly
151 originating from cholesterol, glycerol backbone and fatty acyl chains, therefore attesting for the lipidic
152 rich fraction obtained. The assignment of the 1D NMR signals, achieved both from comparison with
153 literature data (Ekman *et al.*, 2009; Fernando *et al.*, 2011; Jayalakshmi *et al.*, 2011) and the analysis of
154 various lipid standards, is available in Supplementary Material (Supplementary Fig. 2). The
155 repeatability of the extraction protocol was evaluated through the integration of the main observable
156 NMR signals, by drawing large buckets in order to avoid “cutting” overlapping signals which could
157 eventually account for the observed variability. This was followed by normalization on the total sum
158 for each spectrum and calculation of the **Coefficients of Variation (CVs)** across the different replicates
159 for each of these normalized areas (Supplementary Fig. 1, bottom). All resulting CV values were
160 observed below 9%, with only two regions respectively around 3.5 and 1.9 ppm presenting variations
161 above 4%. The value observed for the 3.5 ppm (labeled “k” in Supplementary Material) region is
162 probably due to the low SNR of the associated signal, which accentuates the measurement error. For
163 the 1.9 ppm region (labeled “f”), the high CV can be attributed to the broad water signal around 1.6
164 ppm, caused by an unfortunate water residue in the CDCl₃ bottle used for this experiment. Even if this

165 particular signal was voluntarily discarded for the bucketing, its broad base overlaps the signal
166 integrated in the 1.9 ppm region and therefore influences the CV of this bucketing region.
167 Consequently, a new CDCl₃ bottle was used for all subsequent experiments of the study resulting in no
168 observable water signal thereafter. Apart from those particular cases, the CV values can be deemed as
169 satisfying as they are consistent with repeatability values from the literature. For instance, Pellegrino
170 *et al.* (Pellegrino *et al.*, 2014) tested various methods for serum lipids by LC-MS and obtained optimal
171 values (*ca.* 3% Relative Standard Deviation). Therefore, the proposed extraction method ensures a
172 sufficient repeatability to compare NMR signals, it is also reasonably simple and can be used for high-
173 throughput purposes. However, as both the serum and solvent volumes involved are relatively high
174 compared with an extraction dedicated to MS, particular care is necessary to take the organic phase,
175 without drawing part of the thicker protein layer. Moreover, the stability of the extracts has been
176 verified and resulted in no change in the apparent lipidic fingerprint (superimposed 1D NMR spectra
177 at 128 scans) neither when stored at 277K for one week or stored at 253K for up to 3 weeks; thus
178 validating the use of a 277K autosampler and the storage conditions (253K) of the NMR tubes used
179 between analysis batches. Consequently, we further implemented this protocol to a set of samples
180 selected for its relevance in the present lipidomics context.

181 **3.2 NMR fingerprinting.**

182 For NMR lipidomics, a broad range of 1D and 2D pulse sequences are of potential relevance (Barding
183 *et al.*, 2012; Marchand *et al.*, 2017). 1D ¹³C NMR was initially considered, either through direct
184 detection or polarization transfer experiments, because of the better natural spectral resolution of this
185 nucleus compared to ¹H. Unfortunately, because of limited sample availability, ¹³C NMR spectra of the
186 serum lipid extract at natural abundance could not be recorded with enough sensitivity in a reasonable
187 time. For similar reasons, the use of 2D heteronuclear pulse sequences such as Heteronuclear Single-
188 Quantum Correlation (HSQC) was also discarded.

189 Therefore, we focused on ^1H NMR spectroscopy for optimal sensitivity, testing three different
190 possibilities. Moreover, in order to keep the workflow compatible with high-throughput expectations,
191 an auto-sampler was employed, which can automatically transfer the NMR tubes into the magnet and
192 allows an automatic setting of the shims as described in Supplementary Material. Such procedure
193 allows optimal shim adjustment while keeping limited the human intervention throughout analysis.

194 Firstly, the classical ^1H 1D pulse–acquire sequence was selected because of its recognized high
195 repeatability and reproducibility, as detailed above. However, when lipid extracts are analyzed with
196 this method, significant overlaps are observed between the signals, as can be observed in Fig. 2a.

197 To increase the resolving power without sacrificing the analysis duration, the use of fast 2D NMR
198 approaches was tested. While many fast 2D NMR methods have been described in the literature
199 (Rouger *et al.*, 2017), here this paper focuses on those whose repeatability has already been studied
200 (Le Guennec *et al.*, 2012; Martineau *et al.*, 2013) and whose potential for metabolomics has already
201 been demonstrated, *e.g.* NUS and ultrafast (Jézéquel *et al.*, 2015; Le Guennec *et al.*, 2014). The
202 objective of the present work was not to propose new method optimizations, but rather to evaluate
203 the potential of recently published approaches in the conditions that were previously optimized and
204 published in methodological papers. In 2D NMR, as opposed to 1D, the coefficient of proportionality
205 between the NMR signal (peak volumes) and the analyte concentration depends on numerous
206 parameters such as coupling constants, relaxation times or pulse sequence delays, arising from the
207 multi-pulse nature of 2D NMR experiments. Nevertheless, each individual signal intensity remains
208 directly proportional to the analyte concentration (Giraudeau, 2014). In an untargeted lipidomics
209 framework, this feature ensures the validity of the comparison of a signal from samples of a similar
210 nature. In addition, it has been shown that such 2D spectra used for relative quantification do not need
211 to be recorded with full relaxation between scans, since longitudinal relaxation is only one among
212 numerous factors impacting the peak volume (Giraudeau, 2014). This choice relies on the assumption
213 that relaxation times do not vary significantly between samples of the same nature with small

214 concentration variations. This explains the choice of a short recovery time (4.9 s) to remain compatible
215 with rapid analysis.

216 The first fast 2D NMR approach used in the proposed workflow is the ZQF-TOCSY, acquired with a Non-
217 Uniform Sampling (NUS) scheme. The resulting lipid extract spectra (see Fig. 2b), with 50% NUS, show
218 an important number of signals while keeping a reasonable analysis time of 1 h 47 min (A fully
219 annotated spectrum can be found in Supplementary Fig. 2c). NUS, depending on the way it is used,
220 either allows saving time for a 2D experiment or multiplying the number of points in the indirect
221 dimension, thus enhancing spectral resolution. Le Guennec *et al.* demonstrated the potential of this
222 approach, in the case of the ZQF-TOCSY pulse sequence, for homonuclear 2D NMR metabolomics (Le
223 Guennec *et al.*, 2014). The choice of the ZQF-TOCSY pulse sequence was motivated by the clean in-
224 phase resulting lineshapes and the high number of observable correlations, as illustrated in Fig. 2b. As
225 shown by Le Guennec *et al.*, a 50% level of NUS (resulting in an overall experiment time divided by
226 two) is the optimal choice for ZQF-TOCSY on complex mixtures; higher levels of NUS would result in
227 reconstruction artefacts that could alter the subsequent data extraction and analysis (Le Guennec *et*
228 *al.*, 2015).

229 The second fast 2D approach evaluated in this paper is ultrafast 2D NMR, with a hybrid multi-scan
230 experiment based on the UF COSY sequence. While such experiment has already been used in a
231 metabolomics context (Jézéquel *et al.*, 2015; Le Guennec *et al.*, 2014), this is, to our knowledge, the
232 first time that such an approach is used for lipidomics purposes and the first time it is applied in an
233 automatic way, using an auto-sampler. While UF 2D NMR allows the acquisition of a complete 2D NMR
234 spectrum within a single scan, the sensitivity of sub-second experiments is not suitable for complex
235 samples with realistic concentrations. However, it has been shown that a multi-scan experiment based
236 on UF 2D NMR offers an appealing alternative to conventional NMR for typical experiment durations
237 below 30 minutes (Le Guennec *et al.*, 2012). In these conditions, even if they suffer from the need to
238 compromise between resolution, spectral ~~width~~width and sensitivity (Akoka and Giraudeau, 2015),

239 such hybrid experiments can offer a much higher repeatability than conventional 2D NMR due to their
240 better immunity towards spectrometer instabilities. Indeed, UF spectra are not affected by t_1 noise
241 contrary to their conventional counterparts, and this is a significant advantage for samples with large
242 dynamic ranges (Pathan *et al.*, 2011). Here, we used the UF version of the COSY pulse sequence.
243 Although less information is obtained with COSY sequence compared to ZQF-TOCSY, UF COSY has a
244 much higher sensitivity compared to UF TOCSY –the latter being hampered by the effect of molecular
245 diffusion during the spin-lock period. Indeed, hybrid COSY spectra based on UF spectroscopy yield
246 clean and rich spectra (see Fig. 2c) free of t_1 noise, which facilitates the bucketing step (A fully
247 annotated spectrum can be found in Supplementary Fig. 2d). Moreover, the analysis duration (26 min
248 in the present work, corresponding to the maximum allowed for UF experiments regarding hardware
249 considerations) is much reduced compared to conventional 2D NMR, making such sequence precious
250 for high-throughput applications.

251 **3.3 Application of the workflow to food safety issues**

252 Once this robust workflow was set up, it was applied to study the effect of ractopamine in pigs, and in
253 particular to assess lipids profile disruption in serum upon such treatment. Ractopamine is a synthetic
254 drug belonging to the β -agonist family that may be used as a growth promoter in finishing pigs to
255 promote leaner meat (Ricks *et al.*, 1984). While being authorized in a number of countries worldwide
256 ($n > 25$), it has been banned within the EU since the late 80s (Council Directive 88/146/EEC; Council
257 Directive 96/22/EC). To comply efficiently with such ban, new screening techniques, including
258 untargeted approaches, are expected, to detect any potential abuse (Dervilly-Pinel *et al.*, 2012; Pinel
259 *et al.*, 2010). Untargeted approaches have already proved their efficiency in the bovine species for the
260 detection of urinary specific signatures upon β -agonists treatment (Dervilly-Pinel *et al.*, 2015).
261 Regarding the porcine species, untargeted approaches have not been reported so far in that context,
262 except for a study dealing with the investigation of polar metabolome modifications in the serum as a
263 consequence of ractopamine treatment (Peng *et al.*, 2017). However, as the effect of growth
264 promoters, particularly β -agonists, on the expression of lipids has been studied and reported for a long

265 time (Dunshea, 1993; Dunshea *et al.*, 1998; Soares da Silva Ferreira *et al.*, 2013), it appears that globally
266 investigating lipid profiles through untargeted approach such as lipidomics would be a relevant
267 strategy to generate new knowledge about biological pathways involved. It could also potentially
268 highlight candidate biomarkers that may be further used in a screening context for classification
269 purposes. In this part, results obtained with the three analysis methods (1D, 2D NUS ZQF-TOCSY, 2D
270 UF COSY) are discussed and compared.

271 **1D NMR results.**

272 After application of the workflow, each 1D spectrum was subjected to manual bucketing. As can be
273 seen in Fig. 2a, much overlap is observed on the 1D lipid spectra, in particular in the 0.8 – 2.4 ppm
274 region. Therefore, manual bucketing was optimized in order to prevent, as much as possible, splitting
275 a signal in two different buckets, while drawing a large number of buckets in order to get enough
276 variables for the statistical analysis and subsequent data interpretation. Buckets were first drawn on a
277 superposition of all the spectra, to take potential chemical shift variations into account. These buckets
278 were then applied individually to each spectrum and normalized on the total sum, to ensure
279 comparability of the samples, including QC. Here, the QC are used for setting up shim file as well as
280 assessment of the quality of the analysis. Thus, the data quality was checked by calculating the CVs for
281 each variables across all QC samples. As no bucket presented a $CV_{QC} > 10\%$, all the variables (35 in
282 total) were kept for subsequent statistical analysis. Firstly, a Principal Component Analysis (PCA) on all
283 the samples was performed in order to check the quality of the data, paying particular attention to the
284 QC samples. The PCA score plot showed clustered QCs, illustrating the reproducibility of the analysis
285 during the entire experiment (Supplementary Fig. 4). QCs were then removed for subsequent analyses.
286 As can be expected, samples from days 3 and 9 did not appear different on the PCA score plot between
287 control and treated groups (Supplementary Fig. 5), in accordance with previous findings in bovine
288 reporting a slower response of the lipidome to β -agonist actions compared to metabolome one

289 (Nzougnet *et al.*, 2015). Those time points were then discarded for the rest of the analyses;
290 corresponding PCA is shown in Supplementary Fig. 6.

291 The data were then analyzed with a two-component **partial least squares-discriminant analysis (PLS-**
292 **DA)**, whose score plot is illustrated in Fig. 3a. The first principal component (PC) accounts for 35.8%
293 whereas the second PC accounts for 13.8%. As can be seen in Fig. 3a, a discrimination is observed along
294 the PC1 between the control group (in red) and the treated group (in green). A very good discrimination
295 between sample groups is obtained ($R^2 = 0.84$ and $Q^2 = 0.69$). The robustness of the model for
296 discriminating sample classes was further validated by a permutation test ($n = 100$) –available in
297 Supplementary Fig. 7a– and a CV-ANOVA. The latter resulted in a p-value of 2.6×10^{-5} , thus denoting
298 significance of the model (Eriksson *et al.*, 2008) and the ability of the NMR lipidomics workflow to
299 discriminate sample classes.

300 **2D ZQF-TOCSY results.**

301 The 2D ^1H - ^1H ZQF-TOCSY experiment could potentially improve the quality of the results by spreading
302 the signals into an additional dimension. After processing the spectra, manual bucketing was operated
303 on the 2D peak volumes, by manually drawing rectangular buckets on a 2D contour plot of the spectra.
304 Correlation and diagonal signals were integrated as both contain valuable information; in particular,
305 the information from singlets is only observable on the diagonal. Note that peak overlap was still
306 present in the CH_2 region, albeit to a lesser extent than for 1D spectra. Moreover, t_1 noise, mainly
307 originating from the very intense CH_2 signal of the fatty acyl chains, complicated the bucketing of
308 neighboring signals. Fortunately, as TOCSY provides symmetrical spectra, bucketing could be
309 performed by individually selecting, for each pair of symmetric correlation signals, the one less
310 disturbed by surrounding noise or peak overlap. After normalization on the total sum, a cleaning step
311 similar to the one performed on 1D data was carried out. This step led to the suppression of only 13
312 variables from the dataset which originally contained 153 variables, thus highlighting the good quality
313 of the original data. After checking the quality of the fingerprints by PCA, a two component PLS-DA

314 was performed, from which the score plot is illustrated in Fig. 3b. The first PC explains 38.1% of the
315 variance whereas the second PC explains 11.0%. Samples from both classes could be separated
316 efficiently by the model, as attested by the associated performances ($R^2 = 0.84$ and $Q^2 = 0.71$),
317 permutation tests (Supplementary Fig 6b) and the p-value (3.8×10^{-4}) from the CV-ANOVA. The
318 discrimination performance achieved with this model from 2D spectra is similar to the one achieved
319 with 1D. However, the added value of such 2D fingerprint lies in the additional dimension that reduces
320 signal overlap, leading to a facilitated bucketing step and to the generation of a higher number of
321 variables, which are less affected by peak overlap. This was further confirmed by orthogonal PLS-DA
322 (OPLS-DA), that allow for an easier interpretation of the variable involvement in the discrimination
323 between classes, through loading plot examination. In the associated loading plot from the 1D data,
324 some neighboring overlapping buckets appear close to each other, suggesting similar apparent pattern
325 towards the control/treated status. Fig. 4a illustrates such an example where the bucket attributed to
326 the $-\text{CH}_2\text{-CH}=\text{CH}$ signal from Fatty Acyls (FA) in both buckets n°14 and 15 in the 1D dataset, is merged
327 with the CH (C12) signal from Cholesterol/Esterified cholesterols (Chol/CholE) in bucket n°14 and
328 overlaps with the neighboring CH (C7) from Chol/CholE (bucket n°13). These three buckets are located
329 close to each other in the associated loading plot from OPLS-DA (see Supplementary Fig. 8a). In such
330 cases, doubt still remains about the real relevance of all variables. It is difficult to assess ~~if their~~ if their
331 relative positions on the loading plot arise from a genuine similar biological behavior regarding the
332 control/treated status or are the result of overlapping signals. On the contrary, with 2D data, the
333 corresponding correlation signals can resolve such ambiguity, as the peaks are spread along a second
334 dimension. In Fig 4b from a ZQF-TOCSY spectrum, signals can be separated and integrated according
335 to associated lipid classes. As a consequence, the signal $-\text{CH}_2\text{-CH}=\text{CH}$ from FA (bucket n°27 in the ZQF-
336 TOCSY dataset) can be integrated in a separated bucket from the signals CH (C7) and CH (C12) from
337 Chol/Chol (bucket n°26). Such integration shows that these two variables actually present opposite
338 behavior towards the control/treated status and are located at opposite sides of the associated OPLS-
339 DA loading plot (Supplementary Fig. 8b). Similar occurrences could also be observed, which can be

340 more generally objectivized through examination of the variables loading values according to their
341 positions on the spectra (Supplementary Fig.8). The enhanced and better resolved fingerprint provided
342 by 2D NMR therefore offers an increased confidence in the identification of potential biomarkers and
343 hence in the investigation of lipid metabolism pathways. A similar conclusion was reached in the field
344 of 2D NMR metabolomics (Le Guennec *et al.*, 2014). This result therefore confirms the potential of fast
345 2D ¹H NMR for lipidomics applications.

346 **2D UF COSY.**

347 While the ZQF-TOCSY experiment still suffers from the time penalty inherent to conventional 2D NMR
348 acquisitions, the UF COSY allows to record a 2D spectrum in a time comparable to the one used for 1D
349 spectra. Forty-eight buckets could originally be drawn, resulting in a dataset containing 39 variables
350 after normalization and suppression of buckets with CV_{QC}>10%. This number is comparable to the 35
351 variables of the 1D dataset, but in this case 2D buckets suffer from less signal overlap than in 1D; this
352 is mainly due to the spreading of the signals along a second dimension. Again, the 2D UF COSY dataset
353 was submitted to PLS-DA, after data processing. The resulting PLS-DA score plot (Fig. 3c) shows a
354 similar distribution of the samples compared to 1D and 2D NUS ZQF-TOCSY data, with explained
355 variances of 30.1% for PC 1 and 9.1% for PC 2. This model achieved an efficient discrimination of the
356 two sample classes with R² and Q² values of 0.82 and 0.60 and with confidence parameters associated
357 to the model (p-value from the CV-ANOVA (5.1 x 10⁻⁴), permutation tests (Supplementary Fig. 7c)).
358 Such performance is similar to the one obtained from 1D and ZQF-TOCSY, while the analysis duration
359 remains as low as 26 min. This result can probably be explained by the high repeatability of UF COSY
360 experiments, as previously described in the literature (Akoka and Giraudeau, 2015; Le Guennec *et al.*,
361 2012). The main advantage related to UF COSY is the resolving of ambiguities in the identification of
362 putative biomarkers thanks to the contribution of the second dimension, as explained above for ZQF-
363 TOCSY, with as an acquisition time comparable to the presented 1D experiment and four times faster
364 than the ZQF-TOCSY NUS approach. These results confirm the potential of this technique for lipidomics

365 applications, considering both the relevance of the information provided as well as rapidity of the
366 process. However, it is important to note that the resolution of the observed signals with UF spectra is
367 lower than the NUS spectra and that the COSY sequence only allows to observe correlations between
368 spins which are coupled to each other, as opposed to ZQF-TOCSY, resulting in fewer variables than the
369 latest. Therefore, when one uses the herein presented workflow for lipidomics applications where
370 sample availability is limited, the choice of the selected acquisition approach strongly depends on the
371 desired requirements. If many variables are needed and the number of samples is limited, ZQF-TOCSY
372 NUS appears as a reasonable option. Alternatively, in the case of large-scale applications, where high-
373 throughput is most important, UF COSY would appear as the most appropriate choice.

374 **Biological effects of Ractopamine.**

375 Although the full biological interpretation of our data was not the primary aim of this work, a
376 preliminary interpretation of the effect of Ractopamine on serum lipid profiles in pigs has been carried
377 out, based on the results obtained with the developed workflow. The link between ractopamine and
378 lipid metabolism has been investigated decades ago in farm animals (Dunshea, 1993) and a reduction
379 in the deposition of adipose tissue in the carcass of pigs fed diets containing ractopamine is commonly
380 reported. Such an effect is hypothesized to occur through either reduction in lipogenesis and/or
381 increase in lipolysis and is expected to be reflected in blood through characterization of the lipid
382 profiles disruption, as targeted in the present work.

383 As similar lipids exhibit the same signals on various zones of ^1H NMR spectra, the variables obtained
384 after the bucketing step are rarely unique to one particular lipid. Therefore, this technique does not
385 allow the identification of specific lipid species but rather generally informs on chemical groups or lipid
386 classes, from which qualitative and semi-quantitative variations in observed signals may be the basis
387 for biological interpretation. Consequently, the results from the NUS ZQF-TOCSY dataset were
388 explored, as it contains the highest amount of variables and spectral resolution, facilitating subsequent
389 interpretation. From the PLS-DA described above, the main variables responsible for class separation

390 were extracted using the associated loading plot. Each of these variables was submitted to a Wilcoxon
391 test in order to confirm its discriminative ability, for each time point of this dataset *i.e.* for days 16, 18,
392 23 and 29. Of particular interest for class separation were the variables related to Chol/CholE,
393 phospholipids (PL) and triacylglycerols (TAG) signals. Boxplots for each of these lipid classes can be
394 found in Supplementary Fig.9. Chol/CholE were found to be significant for discrimination between the
395 control and the treated group for day-18, day-29 and marginally significant ($p<0.07$) for day-23. PL
396 were significant for day-29 and marginally significant for day-23 whereas TAG were significant for day-
397 18 and marginally significant for day-23. PL and TAG both presented higher concentrations in samples
398 from treated population, associated to lower Chol/CholE concentrations compared to controlled
399 population. In a recent review, da Sylva Ferreira *et al.* (Soares da Silva Ferreira *et al.*, 2013) went
400 through published studies to understand the *in vivo* mechanism behind the reduction of adipose tissue
401 in carcass of ractopamine-treated animals. In their work, they discussed the two hypothesized
402 pathways in respect of the literature: the reduction in lipogenesis and/or the increase in lipolysis;
403 considering the evaluation of different parameters such as enzymatic activities or quantification of
404 non-esterified fatty acids (NEFA) in porcine blood samples. They concluded on a predominant
405 inhibition of lipogenesis to explain the reduction of lipid deposition on the carcass, rather than a
406 positive effect on lipolysis. Indeed, ractopamine administration is generally not associated with an
407 increase of serum NEFA.

408 Our results suggest lower concentrations of free and esterified cholesterol in pig serum upon the use
409 of ractopamine. The TAG seem to be affected with higher concentrations, yet this was only observed
410 as significant on a short time window (day 18, day 23). The PL were affected in the same way as TAG,
411 albeit at a later stage. The disrupted PL profiles observed in the present study are in accordance with
412 previous observations on muscle where diacylglycerophosphoethanolamine, phosphatidylinositol and
413 sphingomyelin have been associated with ractopamine administration to pigs (Guitton *et al.*, 2017).
414 These observations provide complementary and yet undescribed pieces of information that may
415 contribute to a better understanding of lipid metabolism modifications as a consequence of β -agonist

416 exposure. The full biological investigation of the metabolic and lipidic consequences of β -agonist
417 exposure will be the purpose of future research.

418 **4 Conclusion**

419 In this paper, the development of a robust NMR workflow for untargeted lipidomics, using serum as a
420 matrix, is proposed. First, the repeatability of the sample preparation, using only 300 μ L as sample size,
421 was assessed. Our results demonstrate the ability of the protocol to answer lipidomics requirements
422 in terms of reduced analytical variability. Further, the developed approach proposes, for high-
423 throughput purposes, the innovative combination of automated analysis together with fast ^1H 2D NMR
424 acquisition schemes while keeping a satisfying resolution of the NMR signals. Afterwards, the whole
425 workflow was successfully applied on serum samples collected in the frame of an animal experiment
426 in which disruption of the seric lipid profile was expected within the treated group of animals involved.
427 The observed results confirmed the impact of β -agonists on lipids as already suggested in previous
428 studies in blood (Dunshea and King, 1994), adipose or muscle tissues (Guitton *et al.*, 2017; Reiter *et al.*,
429 2007). Further biological work is currently ongoing to identify the lipids involved and investigate the
430 biological pathways impacted. Despite these encouraging results, further improvements of the
431 approach are still necessary—~~S~~ since several steps of the workflow are still performed manually (sample
432 extraction, data integration). The next step will be ~~targeted~~ dedicated at testing enhanced bucketing
433 approaches, in order to make the best of our data while limiting human intervention, as 2D automatic
434 processing for semi-quantitative approaches emerge in the literature (Puig-Castellvi *et al.*, 2018).
435 Concerning the ractopamine application, our results also showed that further investigations are still
436 necessary for a complete biological understanding. Still, this study highlights the potential of advanced
437 NMR methods for high-throughput lipidomics, thus paving the way towards a better complementarity
438 of NMR and MS in the field. For the analysis of the results and the comparison of the different NMR
439 datasets, the standard PLS-DA was used although the experimental design includes repeated measures
440 on the same animals. For thorough analysis and complete understanding of the biological effects

441 explaining our results, advanced statistical methods suitable for this particular design could be used,
442 such as multilevel methods (Liquet *et al.*, 2012; Westerhuis *et al.*, 2010). Moreover, an appealing
443 perspective is the combination of the described NMR data with MS data, as performed by Marshall et
444 al. for metabolomics (Marshall *et al.*, 2015) in order to optimize the understanding of the effect of
445 Ractopamine.

446 **Acknowledgements**

447 The authors would like to thank the Région Pays de la Loire for funding through the “Recherche-
448 Formation-Innovation: Food 4.2” program (grant LipidoTool).

449 **Compliance with ethical standards**

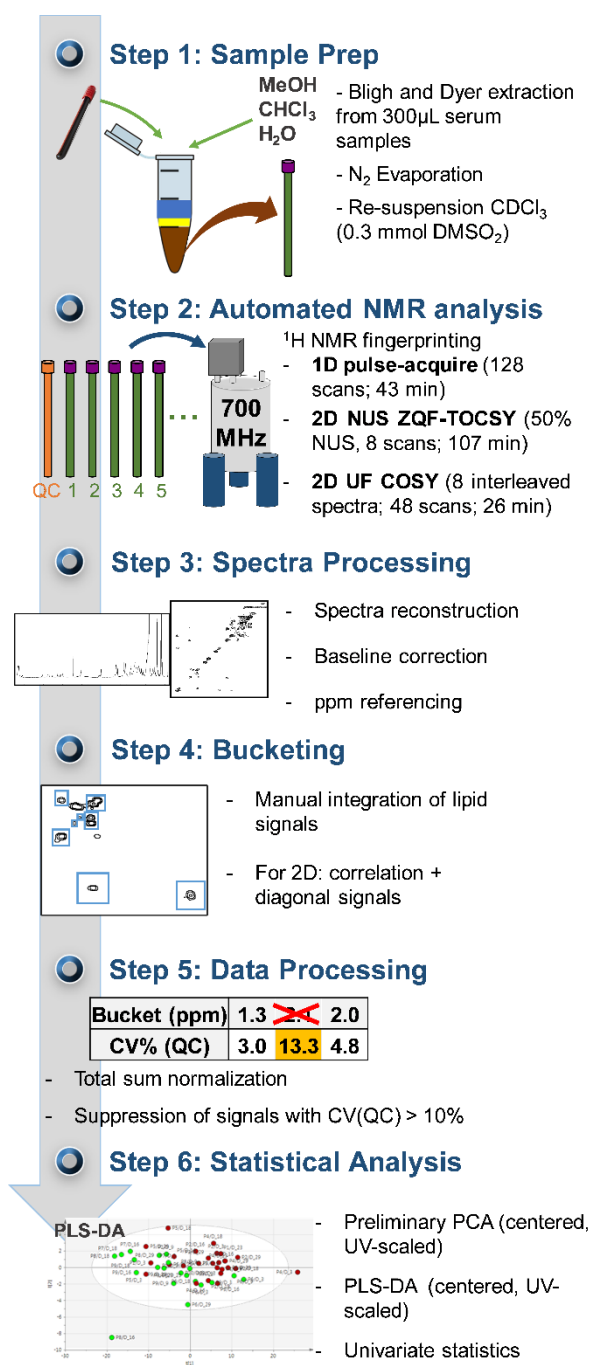
450 **Compliance with animal studies and ethical standards.** The animal study was approved by the national
451 Ethical Committee n°6 (Comité n°6 - Ministère de l’Enseignement Supérieur et de la Recherche –
452 Direction Générale pour la Recherche et l’Innovation – Secrétariat « Autorisation de projet » - 1, rue
453 Descartes, 75231 PARIS cedex 5) under agreement 2,015,092,516,084,715 / APAFIS 1914 (protocol
454 number CRIP-2015-054). The study was implemented at Centre de Recherche et d’Investigation
455 Préclinique-CRIP-ONIRIS- Plate-forme de chirurgie et animaleries expérimentales, Oniris, Nantes,
456 France, under agreement number F.44-271.

457 Institutional and national guidelines were followed for the animal experimentation, as mentioned in
458 Cerfa N° 51706#02 and N° 14906*02; in particular ARTICLES R. 214-87 to 214-137 from CODE RURAL
459 ET DE LA PÊCHE MARITIME (French Regulation).

460 **Conflict of interest.** The authors declare that they have no conflict of interest.

461 **Compliance with ethical requirements.** We confirm that this manuscript has not been published
462 elsewhere and is not under consideration in another journal. All authors have approved the version
463 of this manuscript and agree with its submission to Metabolomics.

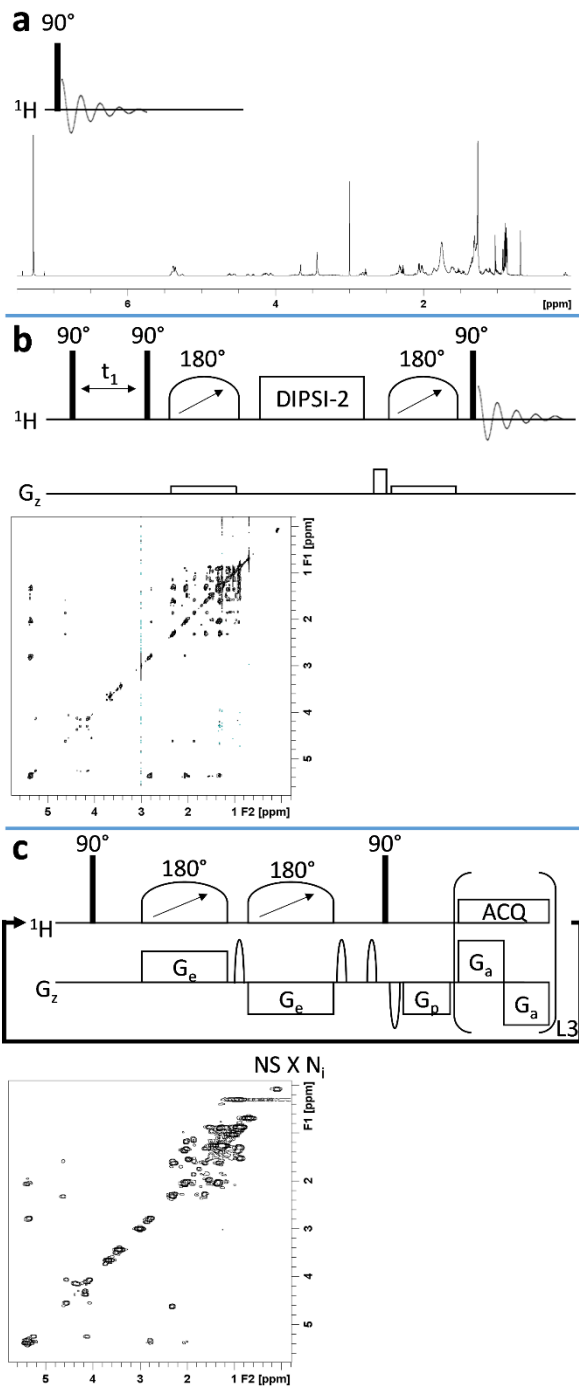
464



465

466

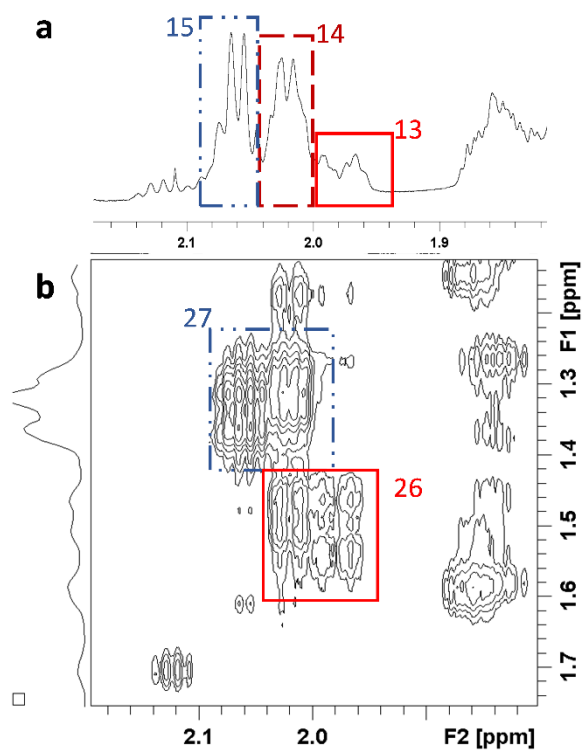
Fig. 1 Schematic of the developed workflow for ¹H NMR lipidomics



467

468 **Fig. 2** ¹H NMR sequences used for lipidomics fingerprinting and associated spectra from pig serum extract. a) 1D Pulse-
 469 acquire. b) 2D ZQF-TOCSY. c) Interleaved multi-scan UF COSY. Spectra recorded at 700 MHz with a cryogenically cooled
 470 probe

471



478

479 **Fig. 4** Zooms on specific bucketing regions in spectra from pig serum lipid extracts. a) Bucketing from a 1D spectrum. The
 480 bucket n°15 contains the $-\text{CH}_2\text{-CH}=\text{CH}$ signal from FA; the bucket n°14 contains both the $-\text{CH}_2\text{-CH}=\text{CH}$ signal from FA and CH
 481 (C12) from Chol/CholE; the bucket n°13 contains the CH (C7) from Chol/CholE. b) Bucketing from a ZQF-TOCSY spectrum. The
 482 bucket n°27 contains the $-\text{CH}_2\text{-CH}=\text{CH}$ signal from FA whereas the bucket n°26 contains the CH (C12) and CH (C7) from
 483 Chol/CholE.

484

485 References

- 486 Akoka, S. and Giraudeau, P. (2015) Fast hybrid multi-dimensional NMR methods based on ultrafast 2D NMR. *Magn. Reson. Chem.* **53**, 986-94.
487
- 488
489 Barding, G.A., Jr., Salditos, R. and Larive, C.K. (2012) Quantitative NMR for bioanalysis and metabolomics. *Anal. Bioanal. Chem.* **404**, 1165-79.
490
- 491
492 Beger, R.D., Schnackenberg, L.K., Holland, R.D., Li, D. and Dragan, Y. (2006) Metabonomic models of human pancreatic cancer using 1D proton NMR spectra of lipids in plasma. *Metabolomics* **2**, 125-134.
493
- 494
495 Bou Khalil, M., Hou, W., Zhou, H., Elisma, F., Swayne, L.A., Blanchard, A.P., Yao, Z., Bennett, S.A. and Figeys, D. (2010) Lipidomics era: accomplishments and challenges. *Mass Spectrom. Rev.* **29**, 877-929.
496
- 497
498 Cajka, T. and Fiehn, O. (2014) Comprehensive analysis of lipids in biological systems by liquid chromatography-mass spectrometry. *TrAC, Trends Anal. Chem.* **61**, 192-206.
499
- 500
501 Council Directive 88/146/EEC Council Directive 88/146/EEC prohibiting the use livestock farming of certain substances having a hormonal action, pp. 16-18.
502
- 503
504 Council Directive 96/22/EC concerning the prohibition on the use in stockfarming of certain substances having a hormonal or thyrostatic action and of beta-agonists, and repealing Directives 81/602/EEC, 88/146/EEC and 88/299/EEC, pp. 3-9.
505
- 506
507 Dervilly-Pinel, G., Chereau, S., Cesbron, N., Monteau, F. and Le Bizec, B. (2015) LC-HRMS based metabolomics screening model to detect various β -agonists treatments in bovines. *Metabolomics* **11**, 403-411.
508
- 509
510 Dervilly-Pinel, G., Courant, F., Chereau, S., Royer, A., Boyard-Kieken, F., Antignac, J. and Le Bizec, B. (2012) Metabolomics in food analysis: application to the control of forbidden substances. *Drug Test. Anal.* **4**, 59-69.
511
- 512
513 Dunshea, F.R. (1993) Effect of metabolism modifiers on lipid metabolism in the pig. *J. Anim. Sci.* **71**, 1966-77.
- 514
515 Dunshea, F.R. and King, R.H. (1994) Temporal response of plasma metabolites to ractopamine treatment in the growing pig. *Aust. J. Agric. Res.* **45**, 1683-1692.
516
- 517
518 Dunshea, F.R., Leur, B.J., Tilbrook, A.J. and King, R.H. (1998) Ractopamine increases glucose turnover without affecting lipogenesis in the pig. *Aust. J. Agric. Res.* **49**, 1147-1152.
519
- 520
521 Ekman, D.R., Teng, Q., Villeneuve, D.L., Kahl, M.D., Jensen, K.M., Durhan, E.J., Ankley, G.T. and Collette, T.W. (2009) Profiling lipid metabolites yields unique information on sex- and time-dependent responses of fathead minnows (Pimephales promelas) exposed to 17 α -ethynylestradiol. *Metabolomics* **5**, 22-32.
522
523
- 524
525 Eriksson, L., Trygg, J. and Wold, S. (2008) CV-ANOVA for significance testing of PLS and OPLS® models. *Journal of Chemometrics* **22**, 594-600.
526
- 527
528 Fernando, H., Bhopale, K.K., Kondraganti, S., Kaphalia, B.S. and Shakeel Ansari, G.A. (2011) Lipidomic changes in rat liver after long-term exposure to ethanol. *Toxicol. Appl. Pharmacol.* **255**, 127-37.
529
- 530
531 Giraudeau, P. (2014) Quantitative 2D liquid-state NMR. *Magn. Reson. Chem.* **52**, 259-72.
532

533 Giraudeau, P. (2017) Challenges and perspectives in quantitative NMR. *Magn. Reson. Chem.* **55**, 61-69.

534

535 Guitton, Y., Dervilly-Pinel, G., Jandova, R., Stead, S., Takats, Z. and Le Bizec, B. (2017) Rapid evaporative ionisation mass spectrometry and chemometrics for high-throughput screening of growth promoters in meat producing animals. *Food Additives & Contaminants: Part A*, 1-11.

537

538

539 Hyotylainen, T., Ahonen, L., Poho, P. and Oresic, M. (2017) Lipidomics in biomedical research-practical considerations. *Biochim. Biophys. Acta* **1862**, 800-803.

540

541

542 Jayalakshmi, K., Sonkar, K., Behari, A., Kapoor, V.K. and Sinha, N. (2011) Lipid profiling of cancerous and benign gallbladder tissues by ¹H NMR spectroscopy. *NMR Biomed.* **24**, 335-42.

543

544

545 Jézéquel, T., Deborde, C., Maucourt, M., Zhendre, V., Moing, A. and Giraudeau, P. (2015) Absolute quantification of metabolites in tomato fruit extracts by fast 2D NMR. *Metabolomics* **11**, 1231-1242.

546

547

548 Le Guennec, A., Dumez, J.N., Giraudeau, P. and Caldarelli, S. (2015) Resolution-enhanced 2D NMR of complex mixtures by non-uniform sampling. *Magn. Reson. Chem.* **53**, 913-20.

549

550

551 Le Guennec, A., Giraudeau, P. and Caldarelli, S. (2014) Evaluation of fast 2D NMR for metabolomics. *Anal. Chem.* **86**, 5946-54.

552

553

554 Le Guennec, A., Tea, I., Antheaume, I., Martineau, E., Charrier, B., Pathan, M., Akoka, S. and Giraudeau, P. (2012) Fast determination of absolute metabolite concentrations by spatially encoded 2D NMR: application to breast cancer cell extracts. *Anal. Chem.* **84**, 10831-7.

555

556

557

558 Lee, H.-C. and Yokomizo, T. (2018) Applications of mass spectrometry-based targeted and non-targeted lipidomics. *Biochemical and Biophysical Research Communications.*

559

560

561 Li, J., Vosegaard, T. and Guo, Z. (2017) Applications of nuclear magnetic resonance in lipid analyses: An emerging powerful tool for lipidomics studies. *Prog. Lipid Res.* **68**, 37-56.

562

563

564 Li, M., Yang, L., Bai, Y. and Liu, H. (2014) Analytical methods in lipidomics and their applications. *Anal. Chem.* **86**, 161-75.

565

566 Liquet, B., Le Cao, K.A., Hocini, H. and Thiebaut, R. (2012) A novel approach for biomarker selection and the integration of repeated measures experiments from two assays. *BMC Bioinf.* **13**, 325.

567

568

569 Malz, F. (2008) Chapter 2 - Quantitative NMR in the Solution State NMR A2 - Holzgrabe, Ulrike in Wawer, I. and Diehl, B. (Eds), *NMR Spectrosc. Pharm. Anal.*, Elsevier, Amsterdam. pp. 43-62.

570

571

572 Marchand, J., Martineau, E., Guitton, Y., Dervilly-Pinel, G. and Giraudeau, P. (2017) Multidimensional NMR approaches towards highly resolved, sensitive and high-throughput quantitative metabolomics. *Curr. Opin. Biotechnol.* **43**, 49-55.

573

574

575 Marshall, D.D., Lei, S., Worley, B., Huang, Y., Garcia-Garcia, A., Franco, R., Dodds, E.D. and Powers, R. (2015) Combining DI-ESI-MS and NMR datasets for metabolic profiling. *Metabolomics* **11**, 391-402.

576

577

578 Martineau, E., Akoka, S., Boisseau, R., Delanoue, B. and Giraudeau, P. (2013) Fast Quantitative ¹H-¹³C Two-Dimensional NMR with Very High Precision. *Analytical Chemistry* **85**, 4777-4783.

579

580

581 Mavromoustakos, T., Zervou, M., Theodoropoulou, E., Panagiotopoulos, D., Bonas, G., Day, M. and Helmis, A. (1997) ¹³C NMR analysis of the triacylglycerol composition of Greek virgin olive oils. *Magn. Reson. Chem.* **35**, S3-S7.

582

583

584 Merchak, N., Silvestre, V., Loquet, D., Rizk, T., Akoka, S. and Bejjani, J. (2017) A strategy for simultaneous determination of
585 fatty acid composition, fatty acid position, and position-specific isotope contents in triacylglycerol matrices by ¹³C-NMR.
586 *Anal. Bioanal. Chem.* **409**, 307-315.

587
588 Nzoughe, J.K., Gallart-Ayala, H., Biancotto, G., Hennig, K., Dervilly-Pinel, G. and Le Bizec, B. (2015) Hydrophilic interaction
589 (HILIC) and reverse phase liquid chromatography (RPLC)–high resolution MS for characterizing lipids profile disruption in
590 serum of anabolic implanted bovines. *Metabolomics* **11**, 1884-1895.

591
592 Pathan, M., Akoka, S., Tea, I., Charrier, B. and Giraudeau, P. (2011) "Multi-scan single shot" quantitative 2D NMR: a valuable
593 alternative to fast conventional quantitative 2D NMR. *Analyst* **136**, 3157-63.

594
595 Pellegrino, R.M., Di Veroli, A., Valeri, A., Goracci, L. and Cruciani, G. (2014) LC/MS lipid profiling from human serum: a new
596 method for global lipid extraction. *Analytical and Bioanalytical Chemistry* **406**, 7937-7948.

597
598 Peng, T., Royer, A.-L., Guitton, Y., Le Bizec, B. and Dervilly-Pinel, G. (2017) Serum-based metabolomics characterization of pigs
599 treated with ractopamine. *Metabolomics* **13**, 77.

600
601 Pinel, G., Weigel, S., Antignac, J.P., Mooney, M.H., Elliott, C., Nielen, M.W.F. and Le Bizec, B. (2010) Targeted and untargeted
602 profiling of biological fluids to screen for anabolic practices in cattle. *TrAC, Trends Anal. Chem.* **29**, 1269-1280.

603
604 Puig-Castellvi, F., Perez, Y., Pina, B., Tauler, R. and Alfonso, I. (2018) Compression of multidimensional NMR spectra allows a
605 faster and more accurate analysis of complex samples. *Chemical Communications* **54**, 3090-3093.

606
607 Reiter, S.S., Halsey, C.H., Stronach, B.M., Bartosh, J.L., Owsley, W.F. and Bergen, W.G. (2007) Lipid metabolism related gene-
608 expression profiling in liver, skeletal muscle and adipose tissue in crossbred Duroc and Pietrain Pigs. *Comp. Biochem. Physiol.,*
609 *Part D: Genomics Proteomics* **2**, 200-6.

610
611 Ricks, C.A., Dalrymple, R.H., Baker, P.K. and Ingle, D.L. (1984) Use of a β -Agonist to Alter Fat and Muscle Deposition in Steers1,
612 *J. Anim. Sci.* **59**, 1247-1255.

613
614 Rouger, L., Gouilleux, B. and Giraudeau, P. (2017) Fast n-Dimensional Data Acquisition Methods A2 - Lindon, John C in Tranter,
615 G.E. and Koppenaal, D.W. (Eds), *Encyclopedia of Spectroscopy and Spectrometry (Third Edition)*, Academic Press, Oxford. pp.
616 588-596.

617
618 Soares da Silva Ferreira, M., Pospissil Garbossa, C.A., Oberlender, G., Pereira, L., Zangeronimo, M., Vicente de Sousa, R. and
619 Cantarelli, V. (2013) Effect of Ractopamine on Lipid Metabolism in vivo - a Systematic Review. *Braz. Arch. Biol. Technol.* **56**,
620 35-43.

621
622 Spener, F., Lagarde, M., G elo en, A. and Record, M. (2003) Editorial: What is lipidomics? *Eur. J. Lipid Sci. Technol.* **105**, 481-
623 482.

624
625 Veenstra, T.D. (2012) Metabolomics: the final frontier? *Genome Med.* **4**, 40.

626
627 Vlahov, G. (1997) Quantitative ¹³C NMR method using the DEPT pulse sequence for the detection of olive oil adulteration
628 with soybean oil. *Magn. Reson. Chem.* **35**, S8-S12.

629
630 Wenk, M.R. (2005) The emerging field of lipidomics. *Nat. Rev. Drug Discovery* **4**, 594-610.

631
632 Wenk, M.R. (2010) Lipidomics: new tools and applications. *Cell* **143**, 888-95.

633
634 Westerhuis, J.A., van Velzen, E.J., Hoefsloot, H.C. and Smilde, A.K. (2010) Multivariate paired data analysis: multilevel PLSDA
635 versus OPLSDA. *Metabolomics* **6**, 119-128.

636

637 Yang, K. and Han, X. (2016) Lipidomics: Techniques, Applications, and Outcomes Related to Biomedical Sciences. *Trends*
638 *Biochem. Sci.* **41**, 954-969.

639

640 Zhao, Y.Y., Wu, S.P., Liu, S., Zhang, Y. and Lin, R.C. (2014) Ultra-performance liquid chromatography-mass spectrometry as a
641 sensitive and powerful technology in lipidomic applications. *Chem.-Biol. Interact.* **220**, 181-92.

642

643